Product Inhibition of the Hepatitis C Virus NS3 Protease

Christian Steinkühler,* Gabriella Biasiol, Mirko Brunetti, Andrea Urbani, Uwe Koch, Riccardo Cortese, Antonello Pessi, and Raffaele De Francesco

Istituto di Ricerche di Biologia Molecolare P. Angeletti (IRBM), Via Pontina Km 30.600, 00040 Rome, Italy

Received February 9, 1998; Revised Manuscript Received April 9, 1998

ABSTRACT: The nonstructural protein NS3 of the hepatitis C virus (HCV) harbors a serine protease domain that is responsible for most of the processing events of the nonstructural region of the polyprotein. Its inhibition is presently regarded as a promising strategy for coping with the disease caused by HCV. In this work, we show that the NS3 protease undergoes inhibition by the N-terminal cleavage products of substrate peptides corresponding to the NS4A−NS4B, NS4B−NS5A, and NS5A−NS5B cleavage sites, whereas no inhibition is observed with a cleavage product of the intramolecular NS3−NS4A junction. The K_i values of the hexamer inhibitory products [K_i(NS4A) = 0.6 μM, K_i(NS5A) = 1.4 μM, and K_i(NS4B) = 180 μM] are lower than the K_m values of the respective substrate peptides [K_m(NS4A−NS4B) = 10 μM, K_m(NS5A−NS5B) = 3.8 μM, and K_m(NS4B−NS5A) > 1000 μM]. Mutagenesis experiments have identified Lys136 as an important determinant for product binding. The phenomenon of product inhibition can be exploited to optimize peptide inhibitors of NS3 protease activity that may be useful in drug development.

The hepatitis C virus (HCV) was identified by molecular cloning in 1989 (*1*). Its genome is a 9.5 kb single-stranded positive sense RNA that contains a single open reading frame encoding a polyprotein of 3010−3033 residues. Upon its synthesis, this polyprotein is processed into at least 10 mature viral proteins. Both cellular signal peptidases and two virally encoded proteolytic enzymes are involved in this maturation process. Whereas the structural HCV proteins arise through the action of cellular proteases (*2*−*5*), the viral enzymes are required for the processing of the nonstructural region. Thus, the NS2−NS3 junction is cleaved by a zinc-dependent autoprotease associated with NS2 and the N-terminal region of the NS3 protein (*6*−*9*). This same region of NS3 also contains a serine protease that performs all remaining cleavages at the intramolecular NS3−NS4A site and at the intermolecular NS4A−NS4B, NS4B−NS5A, and NS5A−NS5B cleavage sites (*3*, *10*−*14*). Besides containing a serine protease domain of about 20 kDa at its N terminus, the NS3 protein harbors an RNA helicase in its ∼400 C-terminal residues (*15*). Deletion experiments have shown that helicase and protease domains can work independently of each other, with the separate polypeptide chains expressing the respective activities (*15*−*22*). This has recently permitted the crystallization of the NS3 protease and helicase domains (*23*−*26*).

Although the NS3 protease has proteolytic activity of its own, in vivo complex formation with the viral NS4A protein is essential for efficient processing of all NS3-dependent polyprotein cleavage sites (*16*, *27*−*29*). NS4A is a cofactor that enhances the specific activity of the NS3 protease and increases its metabolic stability in transfected cells (*27*, *29*). In vitro, NS3 can be activated by addition of a peptide harboring residues 21−34 of the NS4A cofactor. As determined by mutagenesis experiments (*17*, *22*, *28*, *30*, *31*), spectroscopic (*32*) and kinetic studies (*33*), and X-ray crystallography (*23*−*25*), the NS4A cofactor and the peptide derived from it bind to the N-terminal region of the NS3 protease, thereby causing its structural rearrangement and the correct alignment of the residues that constitute the catalytic triad of the enzyme. This process results in the activation of the catalytic machinery.

Substrate specificity studies using peptide substrates based on the sequences of the polyprotein cleavage sites have shown that the NS3 protease requires at least decamer peptides spanning P6−P4′, with a preference for an acidic residue in P6, cysteine in P1, serine or alanine in P1′, and a hydrophobic residue in P4′ (*33*−*35*). Notably, the intramolecular cleavage site between NS3 and its NS4A cofactor differs from this consensus, having threonine as its P1 residue. When incorporated into peptide substrates, this residue has been shown to decrease cleavage efficiency by almost 2 orders of magnitude (*34*), indicating that factors other than maximized cleavage efficiency are operative in selecting for a suboptimal residue in the P1 position of the NS3−NS4A junction.

During our substrate specificity studies, we realized that the NS3 protease is subject to product inhibition. Remarkably, the enzyme displays a higher affinity for the products than it does for the corresponding substrates. In this paper, we present a detailed description of this phenomenon and report evidence for the involvement of Lys136 in the stabilization of the enzyme−product complex. In the following paper in this issue (*36*), we show that very potent competitive inhibitors of HCV serine protease activity can be obtained through single-mutant and combinatorial optimization of NS3 cleavage products.

* To whom correspondence should be adressed. Telephone: +39 6 91093232. Fax: +39 6 91093225. E-mail: Steinkuhler@IRBM.it.

S0006-2960(98)00313-4 CCC: $15.00
Published on Web 06/05/1998

EXPERIMENTAL PROCEDURES

Purification of the NS3 Protease Domain. A plasmid containing the serine protease domain of NS3 (amino acids 1−180, from the HCV J strain, followed by the sequence ASKKKK) cDNA under the control of the bacteriophage T7 gene 10 promoter was used to transform *Escherichia coli* BL21 (DE3) cells. Protein expression and purification were carried out as previously described (*37*). The purity of the enzyme was evaluated to be >95% by silver-stained SDS−polyacrylamide gels and by reversed-phase HPLC using a Vydac C4 column (4.6 × 250 mm, 5 μm, 300 Å). In the latter case, eluents were H_2O/0.1% TFA (A) and acetonitrile/0.1% TFA (B). A linear gradient from 3 to 95% B in 60 min was used. The concentration of protein stocks was estimated by quantitative amino acid analysis. Purified proteins were further characterized by N-terminal sequence analysis, using Edman degradation on an Applied Biosystems model 470A gas-phase sequencer, and by electrospray mass spectrometry with a Perkin-Elmer API 100 instrument. Both techniques indicated an N-terminal heterogeneity of protein samples with 80% of the molecules starting with Met1 and 20% with Pro3.

NS3 Mutants. The Arg155Ser, Lys136Met, and Lys136Arg mutations were inserted by PCR site-directed mutagenesis using suitable primers. cDNAs were fully sequenced and purified proteins analyzed by mass spectrometry to ascertain that no additional mutations were introduced by PCR. The Arg155Ser mutation was inserted in the context of the sequence of the HCV Bk strain protease, since the corresponding J strain mutant turned out to be very poorly expressed in *E. coli*. Control experiments have shown no significant differences in the inhibition of wild-type Bk or J strain proteases by the cleavage products DEMEEC-OH or EDVVAbuC-OH.

Peptides and HPLC Assays. Substrate 4AB, having the sequence Ac-DEMEECASHLPYK-NH_2, was purchased from Peptides International. Substrate 5AB (EDVVAbuCSMSY) was obtained from AnaSpec. Protected amino acids were commercially available from Novabiochem (Läufelfingen, Germany), Bachem (Bubendorf, Germany), Neosystem (Strasburg, Germany), or Synthetech (Albany, NY). Peptide synthesis was performed by Fmoc/t-Bu chemistry (*38*) on Novasyn TGA (peptide acids) or Novasyn TGR (peptide amides) resin. Peptides were purified by HPLC and characterized by mass spectrometry and amino acid analysis. Concentrations of stock solutions of peptides, prepared in DMSO or in buffered aqueous solutions and kept at −80 °C until they were used, were determined by quantitative amino acid analysis performed on HCl-hydrolyzed samples.

If not specified differently, cleavage assays were performed in 57 μL of 50 mM Hepes (pH 7.5), 1% CHAPS, 15% glycerol, and 10 mM DTT (buffer A), to which 3 μL of substrate peptide was added. As the protease cofactor, we used a peptide spanning the central hydrophobic core (residues 21−34) of the NS4A protein, Pep4AK [KKKGSVVIVGRIILSGR(NH_2)]. Buffer solutions containing 80 μM Pep4AK were preincubated for 10 min with 10−200 nM protease, and reactions were started by addition of substrate. Six duplicate data points at different substrate concentrations were used to calculate kinetic parameters. Incubation times were chosen to produce <7% substrate conversion, and reactions were stopped by addition of 40 μL of 1% TFA. Cleavage of peptide substrates was determined by HPLC using a Merck-Hitachi chromatograph equipped with an autosampler. Samples (80 μL) were injected onto a Lichrospher C18 reversed-phase cartridge column (4 × 75 mm, 5 μm, Merck), and fragments were separated using a 10 to 40% acetonitrile gradient at 5%/min using a flow rate of 2.5 mL/min. Peak detection was accomplished by monitoring both the absorbance at 220 nm and tyrosine fluorescence (λ_{ex} = 260 nm, λ_{em} = 305 nm). Cleavage products were quantitated by integration of chromatograms with respect to appropriate standards. Kinetic parameters were calculated from a nonlinear least-squares fit of initial rates as a function of substrate concentration with the help of a Kaleidagraph software, assuming Michaelis−Menten kinetics.

K_i values of peptide inhibitors were calculated from substrate titration experiments performed in the presence of increasing amounts of inhibitor. Experimental data sets were simultaneously fitted to eq 1 using a multicurve fit macro with the help of a Sigmaplot software:

$$V = (V_{max}S)/[K_m(1 + K_i/I) + S] \quad (1)$$

Alternatively, K_i values were derived from IC_{50} values, calculated using a two-parameter logistic function, according to eq 2:

$$IC_{50} = (1 + S/K_m)K_i \quad (2)$$

pH dependence experiments were carried out using a three-component buffer containing 25 mM Tris, 12.3 mM acetate, 12.3 mM Mes, 15% glycerol, 1% CHAPS, 30 mM DTT, and 80 μM Pep4AK. pH-dependent variations of ionic strength were corrected by addition of NaCl such that the final ionic strength of all solutions was 15 mM. Enzymatic reactions using this buffer system were performed as described above. Enzyme concentrations were varied between 500 and 20 nM, and after 30 min, reactions were stopped by addition of 40 μL of 1% TFA.

Molecular Modeling. All computer simulations were performed on a Silicon Graphics Indigo workstation. Energy minimization and molecular dynamics were carried out with the program BatchMin (*39*) and the molecular modeling package InsightII/Discover (Biosym Technologies Inc., San Diego, CA). All hydrogen atoms were included, and the potential energy of the complex was expressed by the force field MMFF (*40*) implemented in the MacroModel V5.0 distribution of the simulation program BatchMin. To approximate solvation, a continuous solvent model for water, as implemented in BatchMin, was employed. Molecular dynamics simulations were performed at 300 K. All atoms of the NS3 protease, except those of the amino acid side chains in the substrate binding region, were kept fixed during the simulation. The MacroModel V5.0 distribution of the simulation program BatchMin was used.

RESULTS

We have analyzed the time course of the NS3-catalyzed cleavage of the substrate peptide DEMEECASHLPYK (substrate 4AB) which is based on the sequence of the NS4A−NS4B cleavage site of the HCV polyprotein. Figure 1 shows that, starting with a substrate concentration of 30

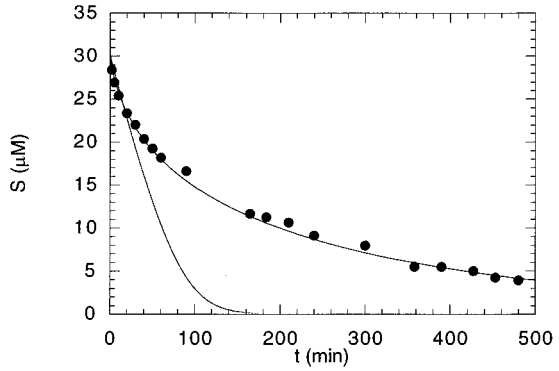

FIGURE 1: Time course of the cleavage of substrate 4AB. NS3 protease (200 nM) was incubated in 50 mM Hepes (pH 7.5), 30 mM DTT, 1% CHAPS, 15% glycerol, and 80 μM Pep4A in the presence of 30 μM substrate 4AB. Aliquots were withdrawn at timed intervals, and the reactions were quenched by addition of 1% TFA and analyzed by HPLC. A theoretical time course of substrate consumption obtained from eq 3, assuming a K_m of 10 μM and a k_{cat} of 2.5 min^{-1}, is shown as a straight line; the ● symbols mark the experimental time course. The experimental time course data have been fitted to eq 4, assuming a K_m of 10 μM and a k_{cat} of 2.5 min^{-1}, the straight line through the data points representing a fit from which a K_i of 0.7 μM has been obtained.

μM ($3K_m$), a considerable deviation from linearity is observed in the time course after only the first 15% of substrate conversion. To investigate the nature of this nonlinearity, K_m and k_{cat} values were determined for the peptide substrate under near-initial rate conditions (<7% substrate conversion). We obtained a K_m of 10 μM and a k_{cat} of 2.5 min^{-1}. These values were used to generate a theoretical time course curve by substituting them into the integrated form of the Michaelis−Menten equation (*41*):

$$V_{max}t = 2.3K_m \log(S_0/S) + (S_0 - S) \quad (3)$$

where $V_{max} = k_{cat}[E]$ and S_0 and S are the substrate concentrations at time zero and time t, respectively. The curve thus generated deviates significantly from the experimental time course curve (Figure 1). Enzyme instability, the simplest explanation for a curvilinear time course, could be ruled out as a cause since preincubation of the protease in buffer for up to 5 h did not significantly affect the specific activity (not shown). The experimental time course data could, however, be fitted with an integrated form of the Michaelis−Menten equation that takes into account the possibility that one of the cleavage products is an inhibitor of the enzyme (*41*) (eq 4):

$$V_{max}t = 2.3K_m[1 + (S_0/K_i)] \log(S_0/S) + [1 - (K_m/K_i)] \times (S_0 - S) \quad (4)$$

where K_i is the dissociation constant of the enzyme−product inhibitor complex. A fit according to eq 4 with a K_m of 10 μM and a V_{max} of 0.5 μM/min is shown in Figure 1. From this fit, we obtained a K_i of 0.7 μM.

Thus, the time course experiments are compatible with the formation, during substrate cleavage by the NS3 protease, of an inhibitory product with a submicromolar K_i value. If this product is competitively inhibiting the enzyme, it can be predicted that the apparent K_m value for substrate 4AB should increase as a function of substrate conversion, whereas k_{cat} should be unaffected. To verify this, substrate titration experiments were made using eight substrate concentrations between 5 and 200 μM. The reactions were stopped at different times. Subsequently, k_{cat} and K_m values were calculated for each experiment. Figure 2A shows that, as expected, the apparent K_m value for substrate 4AB increases with increasing substrate conversion, whereas no significant variation in k_{cat} could be detected. This pattern is compatible with competitive product inhibition and again indicates that deviation from the theoretical time course is not due to enzyme inactivation, which should go along with a decrease in k_{cat}.

To test which of the two fragments arising from NS3-mediated cleavage of substrate 4AB was responsible for the observed inhibition of the enzyme, both were synthesized and tested separately. We found that the C-terminal fragment ASHLPYIEQG did not affect enzymatic activity up to a concentration of 500 μM, whereas the N-terminal cleavage fragment, having the sequence DEMEEC-OH, competitively inhibited NS3 activity with a K_i of 0.6 μM (Figure 2B and Table 1). This figure is consistent with the K_i value of 0.7 μM extrapolated from the fit of eq 2 to the time course data.

We next addressed the question of whether product inhibition is restricted to substrates derived from the sequence of the NS4A−NS4B junction or if it is a general feature of all NS3 substrate sequences. For this purpose, time course experiments like those described above were made using a 10-mer substrate based on the sequence of the NS5A−NS5B cleavage site (substrate 5AB, not shown). Again, a deviation from the theoretical progress curve was observed that was compatible with the formation of an inhibitory product with a K_i of 3 μM. Next, the P side and P′ side fragments of all cleavage sites were analyzed for their inhibitory potency (Table 1). None of the C-terminal fragments, harboring the P′ residues, affected NS3 activity to a significant extent up to a concentration of 300 μM. Conversely, both the hexamer P side fragments of the NS4B−NS5A and of the NS5A−NS5B junctions were micromolar inhibitors of the enzyme. We observed a hierarchy of inhibitory potencies with the NS4A-derived product having the lowest K_i value, the NS5A-derived fragment having an intermediate value, and the NS4B-derived P side hexamer showing the weakest affinity for the enzyme. This order is similar to the ranking of the K_m values for the corresponding substrates (Table 1). In contrast to these data, no inhibition, up to a concentration of 500 μM, was observed with a hexamer fragment corresponding to the P side of the intramolecular cleavage site NS3−NS4A. The lack of inhibition by this peptide could be related to the fact that this is the only sequence containing a threonine in the P1 position (see Discussion).

The P1 α-carboxylate function appears to play a crucial role in determining the potency of the inhibitory P side hexamers. In the case of the 4A-derived sequence DEMEEC-OH, amidation of the P1 α-carboxylate went along with a 130-fold decrease in potency (Table 1). The resulting amide, DEMEEC-NH_2, was still a competitive inhibitor of the NS3 protease. Its affinity for the active site was however 1 order of magnitude weaker than that of the corresponding substrate 4AB.

Inspection of the structure of the active site of the NS3 protease (*25*) reveals the presence of two basic residues, namely, Arg155 and Lys136, in the vicinity of the S1 pocket.

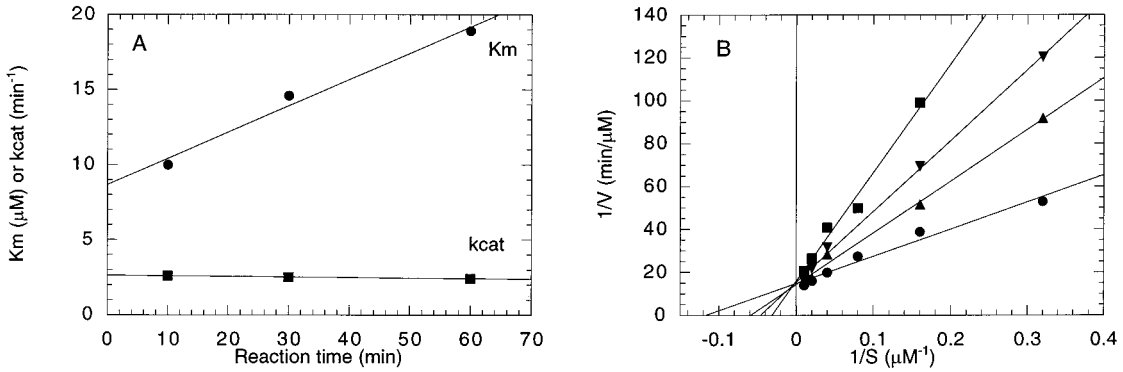

FIGURE 2: (A) Dependence of apparent K_m and k_{cat} values on substrate conversion. Protease (50 nM) was incubated in 50 mM Hepes (pH 7.5), 30 mM DTT, 1% CHAPS, 15% glycerol, and 80 μM Pep4A. The reaction was started by addition of increasing substrate concentrations. After 10, 30, and 60 min, aliquots were withdrawn and the reactions stopped by the addition of 1% TFA. Reactions were analyzed by HPLC, and kinetic parameters were determined as a function of incubation time: (●) apparent K_m value as a function of incubation time and (■) k_{cat} value as a function of incubation time. (B) Lineweaver−Burk analysis of the inhibition of the NS3 protease by its cleavage product DEMEEC-OH. Protease (50 nM) was incubated in 50 mM Hepes (pH 7.5), 30 mM DTT, 1% CHAPS, 15% glycerol, and 80 μM Pep4A (●) or in the same buffer containing 0.5 (▲), 1 (▼), or 2 μM (■) DEMEEC-OH. Reactions were started by addition of increasing amounts of substrate and stopped by the addition of 1% TFA at <7% substrate conversion.

Table 1: Affinity of NS3 Substrates and Their Cleavage Products[a]

peptide	K_m (μM)	K_i (μM)
NS4A−NS4B		
DEMEEC-ASHLPYK-NH_2	10	
DEMEEC-OH		0.6
DEMEEC-NH_2		80
ASHLPYIEQG-NH_2		>500
NS5A−NS5B		
EDVVAbuC-SMSY-NH_2	3.8	
EDVVAbuC-OH		1.4
SMSYTWTGALKK-NH_2		>300
NS4B−NS5A		
DCSTPC-SGSW-NH_2	>1000	
DCSTPC-OH		180
SGSWLRDVWDKK-NH_2		>300
NS3−NS4A		
DLEVVT-STWV	nd	
DLEVVT-OH		>500

[a] All data were determined in the presence of Pep4AK. K_i values were obtained from substrate titration experiments in the presence of increasing inhibitor concentrations, as described in Experimental Procedures, using the substrate peptide 4AB, having the sequence DEMEECASHLPYK. All peptides used were N-terminally acetylated. nd means not determined.

Table 2: Kinetic and Inhibition Parameters of the Arg155Ser and Lys136 Mutants of NS3[a]

			K_i (μM)	
enzyme	K_m (μM)	k_{cat} (min^{-1})	DEMEEC-OH	DEMEEC-NH_2
wild-type	10	2.5	0.6	84
R155S	39	0.2	1.3	nd
K136M	14	0.3	5.0	86
K136R	17	2.0	0.8	70

[a] All reactions were performed in the presence of Pep4AK. Kinetic parameters were determined using substrate 4AB DEMEECASHLPYK. nd means not determined.

These residues could potentially participate in binding to product inhibitors P1 α-carboxylate. Therefore, we decided to mutagenize both and to characterize the effect of these mutations on the affinity of the product inhibitor DEMEEC-OH.

Arg155 was mutagenized into serine, since most chymotrypsin-like serine proteases contain this residue in the homologous position. The Arg155Ser mutation affected both k_{cat} and K_m values for the substrate 4AB (Table 2). In contrast, only a small (2-fold) effect of this mutation was observed on the potency of product inhibitor DEMEEC-OH. The ratio $K_{m(substrate)}/K_{i(DEMEEC-OH)}$, which is a measure of the relative extent of product inhibition, increased from 16.6 to 30, indicating that this mutation slightly strengthened the interaction with DEMEEC-OH relative to substrate binding.

Mutagenesis of Lys136 into methionine also affected the catalytic efficiency of the enzyme, resulting in decreased k_{cat} and slightly increased K_m values for substrate 4AB (Table 2). Furthermore, the mutation led to an 8.3-fold increase in the K_i value of DEMEEC-OH, whereas the K_i for the amide analogue DEMEEC-NH_2 was unaffected (Table 2). The ratio $K_{m(substrate)}/K_{i(DEMEEC-OH)}$, decreased from 16.6 in the wild-type enzyme to 2.8 in the Lys136Met mutant, implying that, in contrast to Arg155, Lys136 is selectively contributing to the stabilization of the bound product inhibitor. Time course curves recorded with the Lys136Met mutant were compatible with an inhibition of this enzyme by DEMEEC-OH with a K_i of 3 μM (not shown), a value similar to that obtained in direct DEMEEC-OH titration experiments (5 μM). To further test the hypothesis that a positively charged residue in position 136 is involved in binding the product P1 α-carboxylate, Lys136 was also mutagenized into arginine. This mutation yielded an enzyme with both kinetic and inhibition parameters that were very similar to those of the wild-type enzyme (Table 2), implying that a positively charged residue in position 136 is important for both catalytic efficiency and product binding.

To characterize further the phenomenon of product inhibition, pH dependence experiments of substrate and product binding were performed. Binding of the substrate 4AB as a function of pH is shown in Figure 3A. The K_m value of this substrate titrates with a pK_a of <5 and varies little between pH 7 and 9. We compared this behavior to the pH dependence of the K_i value of the inhibitors DEMEEC-NH_2 and DEMEEC-OH. The K_i value of DEMEEC-NH_2 was relatively invariant between pH 6 and 8.5, which resembles the behavior of the substrate (Figure 3B). In contrast, there was a striking increase in the K_i value of DEMEEC-OH above pH 7.5 (Figure 3B). The titration data of this product inhibitor were thus compatible with the interaction of the

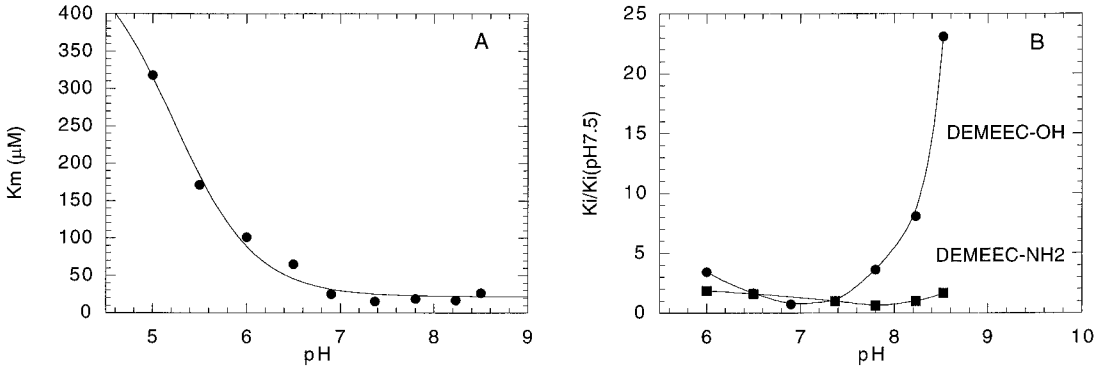

FIGURE 3: pH dependence of substrate 4AB and inhibitor binding to the NS3 protease. Protease (20−500 nM) was incubated in a three-component buffer containing 25 mM Tris, 12.3 mM acetate, 12.3 mM Mes, 15% glycerol, 1% CHAPS, 30 mM DTT, and 80 μM Pep4AK, adjusted to a final pH between 5.0 and 8.6. (A) Titration experiments were performed with substrate 4AB, and K_m values were calculated as a function of pH. (B) K_i values for the inhibitors DEMEEC-OH and DEMEEC-NH_2 were calculated at different pH values from titration experiments performed at [S] = K_m. Due to the different affinities of the two compounds, K_i values at pH 7.5 were normalized to 1, to superimpose both curves on the same graph.

DEMEEC-OH P1 α-carboxylate with a group on the enzyme having a pK_a of >8.5. The exact determination of this pK_a value proved to be difficult due to a decreased stability of the enzyme at high pH values. It can be concluded, however, that the deprotonation of this group selectively destabilizes the interaction with DEMEEC-OH, but not with DEMEEC-NH_2, which indicates that it is probably directly interacting with the P1 α-carboxylate in the product inhibitor. pH dependence experiments performed with the Lys136Met mutant indicated that also in the absence of a positively charged residue in position 136 the affinity for DEMEEC-OH decreased with increasing pH (not shown), suggesting that some other titratable group(s) besides Lys136 contributes to the stabilization of the bound inhibitor.

Energy minimization and molecular dynamics were further used to explore the possible interactions between the product inhibitor and the active site of the NS3 protease. Modeling different side chain conformations of the amino acids close to the active site revealed stabilizing interactions between the side chain of Lys136, which is is located next to the oxyanion hole, and the carboxylic acid moiety of the product inhibitor DEMEEC-OH. Hydrogen bond interactions between the Lys136 side chain and the carboxylic acid oxygen atoms can be achieved by minor changes of the side chain conformation of this residue (Figure 4). In modeling studies using a continuous water model, this interaction seems to contribute significantly to the stabilization of negatively charged groups bound to the active site. The reduction of the distance between the anionic group of the inhibitor and the positively charged Lys side chain is associated with a weakening of the hydrogen bonds between the carboxylic acid and the Ser139 amide group. Additional hydrogen bonds, typical for the oxyanion hole of serine proteases, can be formed between Ser139, Gly137, His57, and the oxygen atoms of the carboxylic acid.

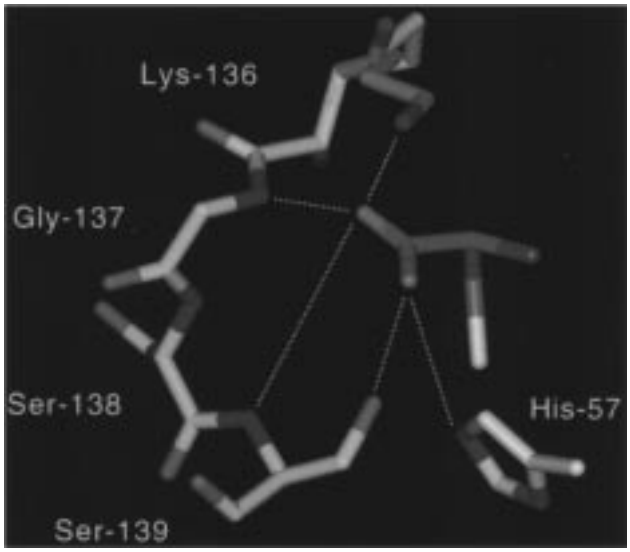

FIGURE 4: Representation of the X-ray structure of the oxyanion hole including the catalytic His57 and Lys136 with the P1 amino acid (Cys) of a product inhibitor modeled into the active site of the NS3 protease. The carbon atoms of the amino acids taken from the X-ray crystal structure are presented in gray and those of the P1 Cys in green. The modeled side chain conformation of Lys136 in the complex with the product inhibitor is shown in pink.

DISCUSSION

Product inhibition of serine proteases, to the extent observed with the NS3 protease, is unusual. In general, serine proteases may be inhibited by high millimolar concentrations of their C-terminal cleavage products for thermodynamic reasons, the free amino group acting as a nucleophile in an acyl transfer reaction (*42*). This mode of inhibition clearly differs from the mechanism of product inhibition observed with the NS3 protease, where the N-terminal cleavage products bind to the enzyme with low micromolar affinities, comparable to or higher than those of the corresponding substrates. Amidation of the P1 α-carboxylate as well as a series of other chemical modifications [see the following paper in this issue (*36*)] has highlighted the importance of the contribution of this acidic group to the overall affinity of NS3 product inhibitors. The interactions of this group with the active site of the protease have therefore attracted our interest.

A series of complexes of serine proteases and their N-terminal cleavage products have been crystallized (*43*−*47*). There is a common binding motif that stabilizes the P1 α-carboxylate function in its enzyme-bound state; in the Sindbis Virus core protein (*47*), the streptomyces griseus protease A (SGPA) complexed with tetramer product peptides (*44*) and in bovine thrombin complexed with a tetradecapeptide mimicking the Aα chain of human fibrino-

gen (*45*) the P1 α-carboxylate oxygens are positioned to make hydrogen bonds with the imidazole ring of the catalytic histidine and with the main chain amido groups of the residues of the oxyanion hole. For SGPA, it has furthermore been proposed that the O^{γ} of the catalytic Ser195 which is very close (2.62 Å) to the carboxyl carbon atom of the product actually is engaged in a partial bond with this atom (*44*). A close contact between these two groups is also observed in the thrombin−tetradecapeptide complex (*45*). The main stabilization of the SGPA−product complexes was postulated to arise from a hydrogen bond between $N^{\epsilon 2}$ of the catalytic His57 and the terminal oxygen atom of the product. This stabilization relies on the protonation of His57 at the low pH (4.1) used to grow the crystals and would be lost upon raising the pH above 7. Under these conditions, not only hydrogen bond formation but also an ion pair electrostatic stabilization of the protonated imidazole and the carboxylate group would be lost. We reasoned that, if such an interaction was making a crucial contribution to the stabilization of the NS3−product complexes, a change in the protonation state of His57 of NS3 should affect the affinity for the product, whose K_i value should titrate with the pK_a value of His57. This pK_a value has previously been determined, both by activity titration (manuscript in preparation) and by NMR titration of the His57 proton resonances (*48*), to be 6.9. Our experimental data indicated instead that the product P1 α-carboxylate was stabilized by the interaction with the protonated form of a group having a pK_a of >8.5. In principle, this finding per se does not exclude His57 as an interacting residue. In fact, the pK_a value of the catalytic histidine of chymotrypsin in complexes with trifluoromethyl ketones has been shown to be >10 (*49*), indicating that we might also be titrating a pK_a value alteration of His57, due to complex formation with the product inhibitor. The exact binding mode of NS3 protease product inhibitors will have to be determined by X-ray crystallography.

Our mutagenesis experiments pointed to Lys136 as a residue that was contributing to the stabilization of the interaction with the P1 α-carboxylate. This conclusion was based on the observation of a loss of inhibitory potency of DEMEEC-OH, but not of the corresponding amide, in the Lys136Met mutant compared to the unaltered potency of DEMEEC-OH in the Lys136Arg mutant. Also, the Lys136Met mutant enzyme showed a pH-dependent decrease in the inhibitory potency of DEMEEC-OH at pH >7.5, indicating that, although being important, Lys136 was not the sole titratable group involved in the stabilization of the bound product. Also, Lys136 is not the sole determinant for discrimination between DEMEEC-OH and DEMEEC-NH_2 as judged from the preference of product with respect to amide binding in the Lys136Met mutant. Our modeling studies suggested that the oxygen atoms of the carboxylic acid of the product inhibitor may engage in hydrogen bond formation with His57 and residues Ser139 and Gly137 of the oxyanion hole of NS3. From molecular dynamics calculations, it was concluded that the interaction between the side chain of Lys136 and the carboxylic acid moiety of the product inhibitor goes along with a weakening of the interaction with the amide group of Ser139. This suggests that in the Lys136Met mutant alternative binding modes involving stronger interactions with the oxyanion hole amide functionalities or with the catalytic histidine might be operative in selectively stabilizing the bound carboxylic acid with respect to the amide, thereby partially compensating for the loss of a positively charged side chain in position 136.

This stabilization of a serine protease−product complex through interaction with a lysine residue at the active site has also been observed in thrombin−tripeptide product complexes (*46*). Thus, in the thrombin−D-Phe-Pro-Arg-OH complex, the P1 α-carboxylate is accepting a hydrogen bond from the $N^{\epsilon 2}$ of the catalytic His57 as well as from an ordered solvent molecule. This ordered solvent is in turn hydrogen-bonded to Lys60F−Nγ. Furthermore, in the Sindbis protease, an arginine residue is conserved in a position similar to that of Lys136 in NS3. In line with this finding, our data on the Lys136Arg mutant show that in NS3 arginine can substitute for lysine in product binding.

The question of whether product inhibition of the NS3 protease has any physiological relevance is still open for debate. In this context, it is interesting to notice that in the intramolecular cleavage site between NS3 and NS4A, at variance with the substrate preference of the protease, a threonine residue is conserved in all isolates. On the other hand, we have shown that the resulting cleavage product does not inhibit the enzyme to any significant extent. If product inhibition does play a role also during polyprotein processing, it could be argued, in the light of these findings, that its occurrence at the intramolecular site should be counter-selected since it may impede subsequent cleavages.

We have noticed that product inhibition is very sensitive to ionic strength [see also the following paper in this issue (*36*)]. In this respect, binding of products parallels the previously reported ionic strength dependence of substrate binding (*50*). This observation is also in line with a predominantly electrostatic stabilization of the enzyme−product complex. In the following paper in this issue (*36*), we show that product inhibitors of the NS3 protease can be optimized to yield peptidic inhibitors with nanomolar potencies which also show reduced sensitivity to ionic strength. These molecules may be useful in the design of peptidomimetics with therapeutical potential as anti-HCV drugs.

ACKNOWLEDGMENT

We thank S. Acali for peptide synthesis, R. Petruzzelli for N-terminal sequence analysis, and F. Naimo and F. Bonelli for mass spectrometry of protein samples.

REFERENCES

1. Choo, Q. L., Kuo, G., Weiner, A. J., Overby, L. R., Bradley, D. W., and Houghton, M. (1989) *Science 244*, 359−362.
2. Hijikata, M., Kato, N., Ootsuyama, Y., Nakagawa, M., and Shimotohno, K. (1991) *Proc. Natl. Acad. Sci. U.S.A. 88*, 5547−5551.
3. Hijikata, M., Mizushima, H., Tanji, Y., Komoda, Y., Hirowatari, Y., Akagi, T., Kato, N., Kimura, K., and Shimotohno, K. (1993) *Proc. Natl. Acad. Sci. U.S.A. 90*, 10773−10777.
4. Shimotohno, K., Hirowatari, Y., Komoda, Y., Kato, N., and Hijikata, M. (1995) *J. Hepatol. 22* (Suppl. 1), 87−92.
5. Santolini, E., Pacini, L., Fipaldini, C., Migliaccio, G., and La Monica, N. (1995) *J. Virol. 69*, 7461−7471.
6. Grakoui, A., McCourt, D. W., Wychowski, C., Feinstone, S. M., and Rice, C. M. (1993) *Proc. Natl. Acad. Sci. U.S.A. 90*, 10583−10587.

7. Hijikata, M., Mizushima, H., Akagi, T., Mori, S., Kakiuchi, N., Kato, N., Tanaka, T., Kimura, K., and Shimotohno, K. (1993) *J. Virol. 67*, 4665−4675.
8. Pieroni, L., Santolini, E., Fipaldini, C., Pacini, L., Migliaccio, G., and La Monica, N. (1997) *J. Virol. 71*, 6373−6380.
9. Santolini, E., Migliaccio, G., and La Monica, N. (1994) *J. Virol. 68*, 3631−3641.
10. Bartenschlager, R., Ahlborn-Laake, L., Mous, J., and Jacobsen, H. (1993) *J. Virol. 67*, 3835−3844.
11. Eckard, M. R., Selby, M., Masiarz, F., Lee, C., Berger, K., Crawford, K., Kuo, C., Kuo, G., Houghton, M., and Choo, Q. L. (1993) *Biochem. Biophys. Res. Commun. 192*, 399−406.
12. Grakoui, A., McCourt, D. W., Wychowski, C., Feinstone, S. M., and Rice, C. M. (1993) *J. Virol. 67*, 2832−2843.
13. Komoda, Y., Hijikata, M., Tanji, Y., Hirowatari, Y., Mizushima, H., Kimura, K., and Shimotohno, K. (1994) *Gene 145*, 221−226.
14. Tomei, L., Failla, C., Santolini, E., De Francesco, R., and La Monica, N. (1993) *J. Virol. 67*, 4017−4026.
15. Kim, D. W., Gwack, Y., Han, J. H., and Choe, J. (1995) *Biochem. Biophys. Res. Commun. 215*, 160−166.
16. Bartenschlager, R., Ahlborn-Laake, L., Mous, J., and Jacobsen, H. (1994) *J. Virol. 68*, 5045−5055.
17. Failla, C., Tomei, L., and De Francesco, R. (1995) *J. Virol. 69*, 1769−1777.
18. Tanji, Y., Hijikata, M., Hirowatari, Y., and Shimotohno, K. (1994) *J. Virol. 68*, 8418−8422.
19. Han, D. S., Hahm, B., Rho, H. M., and Jang, S. K. (1995) *J. Gen. Virol. 76*, 985−993.
20. Kolykhalov, A. A., Feinstone, S. M., and Rice, C. M. (1994) *J. Virol. 68*, 7525−7533.
21. Preugschat, F., Averett, D. R., Clarke, B. E., and Porter, D. J. T. (1996) *J. Biol. Chem. 271*, 24449−24457.
22. Steinkühler, C., Tomei, L., and De Francesco, R. (1996) *J. Biol. Chem. 271*, 6367−6373.
23. Kim, J. L., Morgenstern, K. A., Lin, C., Fox, T., Dwyer, M. D., Landro, J. A., Chambers, S. P., Markland, W., Lepre, C. A., O'Malley, E. T., Harbeson, S. L., Rice, C. M., Murcko, M. A., Caron, P. R., and Thomson, J. A. (1996) *Cell 87*, 343−355.
24. Love, R. A., Parge, H. E., Wickersham, J. A., Hostomsky, Z., Habuka, N., Moomaw, E. W., Adachi, T., and Hostomska, Z. (1996) *Cell 87*, 331−342.
25. Yan, Y., Li, Y., Munshi, S., Sardana, V., Cole, J., Sardana, M., Steinkühler, C., Tomei, L., De Francesco, R., Kuo, L., and Chen, Z. (1998) *Protein Sci. 7*, 837−847.
26. Yao, N., Hesson, T., Cable, M., Hong, Z., Kwong, A. D., Le, H. V., and Weber, P. C. (1997) *Nat. Struct. Biol. 4*, 463−467.
27. Failla, C., Tomei, L., and De Francesco, R. (1994) *J. Virol. 68*, 3753−3760.
28. Lin, C., Thomson, J. A., and Rice, C. M. (1995) *J. Virol. 69*, 4373−4380.
29. Tanji, Y., Hijikata, M., Satoh, S., Kaneko, T., and Shimotohno, K. (1995) *J. Virol. 69*, 1575−1580.
30. Shimizu, Y., Yamaji, K., Masuho, Y., Yokota, T., Inoue, H., Sudo, K., Satoh, S., and Shimotohno, K. (1996) *J. Virol. 70*, 127−132.
31. Tomei, L., Failla, C., Vitale, R. L., Bianchi, E., and De Francesco, R. (1996) *J. Gen. Virol. 77*, 1065−1070.
32. Bianchi, E., Urbani, A., Biasiol, G., Brunetti, M., Pessi, A., De Francesco, R., and Steinkühler, C. (1997) *Biochemistry 36*, 7890−7897.
33. Landro, J. A., Raybuck, S. A., Luong, Y. P. C., O'Malley, E. T., Harbeson, S. L., Morgenstern, K. A., Rao, G., and Livingston, D. J. (1997) *Biochemistry 36*, 9340−9348.
34. Urbani, A., Bianchi, E., Narjes, F., Tramontano, A., De Francesco, R., Steinkühler, C., and Pessi, A. (1997) *J. Biol. Chem. 272*, 9204−9209.
35. Zhang, R., Durkin, J., Windsor, W. T., McNemar, C., Ramanathan, L., and Le, H. V. (1997) *J. Virol. 71*, 6208−6213.
36. Ingallinella, P., Altamura, S., Bianchi, E., Taliani, M., Ingenito, R., Cortese, R., De Francesco, R., Steinkühler, C., and Pessi, A. (1998) *Biochemistry 37*, 8906−8914.
37. De Francesco, R., Urbani, A., Nardi, M. C., Tomei, L., Steinkühler, C., and Tramontano, A. (1996) *Biochemistry 35*, 13282−13287.
38. Atherton, E., and Sheppard, R. C. (1989) *Solid-phase peptide synthesis. a practical approach*, IRL Press, Oxford, U.K.
39. Mohamadi, F., Richards, N. G., Guida, W. C., Liskamp, R., Liptom, M., Caufield, C., Chang, G., Hendrickson, G., and Still, W. C. (1990) *J. Comput. Chem. 11*, 440−467.
40. Halgren, T. A. (1996) *J. Comput. Chem. 17*, 490−519.
41. Segel, I. H. (1993) *Enzyme Kinetics*, John Wiley & Sons, Inc., New York.
42. Schellenberger, V., Turck, C., and Rutter, W. J. (1994) *Biochemistry 33*, 4251−4257.
43. Choi, H. K., Tong, L., Minor, W., Dumas, P., Boege, U., Rossmann, M. G., and Wengler, G. (1991) *Nature 345*, 37−43.
44. James, M. N. G., Sielecki, A. R., Brayer, G. D., and Delbaere, L. T. J. (1980) *J. Mol. Biol. 144*, 43−88.
45. Martin, P. D., Robertson, W., Turk, D., Huber, R., Bode, W., and Edwards, B. F. P. (1992) *J. Biol. Chem. 267*, 7911−7920.
46. Nienaber, V. L., Mersinger, L. J., and Kettner, C. A. (1996) *Biochemistry 35*, 9690−9699.
47. Tong, L., Wengler, G., and Rossmann, M. G. (1993) *J. Mol. Biol. 230*, 228−247.
48. Urbani, A., Bazzo, R., Nardi, M. C., Cicero, D., De Francesco, R., Steinkühler, C., and Barbato, G. (1998) *J. Biol. Chem.* (in press).
49. Cassidy, C. S., Lin, J., and Frey, P. (1997) *Biochemistry 36*, 4576−4584.
50. Steinkühler, C., Urbani, A., Tomei, L., Biasiol, G., Sardana, M., Bianchi, E., Pessi, A., and De Francesco, R. (1996) *J. Virol. 70*, 6694−6700.

BI980313V